ISSN 1027-5495. Functional Materials, 28, No.2 (2021), p. 359-365.
doi:https://doi.org/10.15407/fm28.02.359

Prediction of carbide liquidus and carbide composition of the Ni–14Cr–9Co–5Ti–3Al–3Ta–3.5W–1.5Mo–0.15Hf–0.1C system

***V.E.Ol'shanetskii*[1], *A.A.Glotka*[1], *V.V.Klochikhin*[2]**

[1]Zaporizhzhia Polytechnic National University,
64 Zhukovskogo Str., 69063 Zaporizhzhia, Ukraine
[2]JSC "MOTOR SICH", 15 Motorobudivnukiv Str.,
69068 Zaporizhzhia, Ukraine

Received December 4, 2020

The specificity of the distribution of alloying elements in carbides of the multicomponent system Ni–14Cr–9Co–5Ti–3Al–3Ta–3.5W–1.5Mo–0.15Hf–0.1C has been studied. The CALPHAD method was used to simulate the thermodynamic processes of crystallization. The dependences of the influence of alloying elements on the temperatures of dissolution (precipitation) of carbides are obtained. The results of thermodynamic calculations of the chemical composition of carbides are presented in comparison with the experimental data obtained by electron microscopy on a microscope REM-106I with a system of energy-dispersive X-ray spectral microanalysis. It is shown that the dependences obtained are closely correlated with thermodynamic processes occurring in the system.

Keywords: nickel-based superalloys of directional solidification, alloying system, CALPHAD method, structure, composition of carbides.

Прогнозування карбідного ліквідусу і складу карбідів системи Ni–14Cr–9Co–5Ti–3Al–3Ta–3.5W–1.5Mo–0.15Hf–0.1C. *В.Ю.Ольшанецький, О.А.Глотка, В.В.Клочихін*

Вивчено специфіку розподілу легувальних елементів у карбідах багатокомпонентної системи Ni–14Cr–9Co–5Ti–3Al–3Ta–3.5W–1.5Mo–0.15Hf–0.1C. Методом CALPHAD проведено моделювання термодинамічних процесів кристалізації. Отримано залежності впливу легувальних елементів на температури розчинення (виділення) карбідів. Результати термодинамічних розрахунків хімічного складу карбідів наведено у порівнянні з експериментальними даними, отриманими методом електронної мікроскопії на мікроскопі РЕМ-106И з системою енергодисперсійного рентгеноспектрального мікроаналізу. Показано, що отримані залежності тісно корелюють з термодинамічними процесами, що відбуваються у системі.

Изучена специфика распределения легирующих элементов в карбидах многокомпонентной системы Ni–14Cr–9Co–5Ti–3Al–3Ta–3.5W–1.5Mo–0.15Hf–0.1C. Методом CALPHAD проведено моделирование термодинамических процессов кристаллизации. Получены зависимости влияния легирующих элементов на температуры растворения (выделения) карбидов. Результаты термодинамических расчетов химического состава карбидов приведены в сравнении с экспериментальными данными, полученными методом электронной микроскопии на микроскопе РЭМ-106И с системой энергодисперсионного рентгеноспектрального микроанализа. Показано, что полученные зависимости тесно коррелируют с термодинамическими процессами, происходящими в системе.

1. Introduction

The addition of carbon to nickel-based superalloys in an amount of 0.05 to 0.2 % and carbide-forming elements promotes the precipitation of carbides of the $M_{23}C_6$, MC, and M_6C types. These carbide phases are unstable and, under the influence of temperature and time of operation, they can undergo transformations, changing the form, size and morphology, which affect the properties of the alloys at high temperatures [1]. Precipitations of carbide phases play an important role in the mechanical properties of superalloys [2–5]. Discrete carbide particles precipitating at the grain boundaries can inhibit slip and improve the strength and creep resistance of the alloy at elevated temperatures. $M_{23}C_6$ carbides resist sliding along grain boundaries for improved creep resistance. The morphology of these carbides has a significant effect on the properties of nickel-based alloys. The sequence of formation, composition and morphological evolution of MC carbide depending on the solidification rate, have been described in numerous works [6–12]. In general, the morphology of MC carbides in a cast nickel-base alloy depends on its composition and casting parameters, because this type of carbide is formed during solidification. MC carbides can degrade to form M_6C and / or $M_{23}C_6$ carbides during operation or heat treatment, thus the size, morphology and type of carbide can be altered by heat treatment of the alloy.

The purpose of this work is to obtain mathematical models for predicting the temperatures of carbide liquidus and the composition of carbide phases for a multicomponent system such as Ni–14Cr–9Co–5Ti–3Al–3Ta–3.5W–1.5Mo–0.15Hf–0.1C using the computational prediction method CALPHAD (passive experiment) versus electron microscopy data (active experiment).

2. Experimental

Modeling of thermodynamic processes occurring in the structure of alloys during crystallization (cooling) or heating was carried out by the CALPHAD [13] method in the temperature range of 1600–20°C with directional crystallization.

In the multicomponent alloying system (Ni–14Cr–9Co–5Ti–3Al–3Ta–3.5W–1.5Mo–0.15Hf–0.1C), the range of changes in the content of the element was chosen based on considerations of the maximum and minimum amount of the element introduced into heat-resistant nickel alloys (ZHNS). Thus, for the study, carbide-forming elements were selected in the following alloying ranges (% by weight): carbon 0.02–0.2; titanium 1–6; tantalum 0.5–12; chrome 1–35; molybdenum 1–6; tungsten 1–16; hafnium 0.1–2.5.

Experimentally, the composition of carbides was determined on a REM-106I electron microscope using an energy-dispersive X-ray spectral microanalysis system. This method was used to study the morphology and chemical composition of precipitated carbides in the alloy structure. Conversion of qualitative values for quantitative analysis was performed automatically according to the program of the device. The relative error of the method is ±2 % (by weight). The calculation results on the type of carbides and their chemical composition were compared with the experimental data obtained using electron microscopy.

The results of the study were processed in the Microsoft Office software package in the EXCEL package with the establishment of correlation dependences of the "parameter-property" type in the form of mathematical equations for mathematical models that optimally describe these dependences. The obtained dependences have rather high coefficients of the correlation criterion $R^2 \geq 0.85$ and can be used for predictive calculations of the indicated characteristics with a relative error of the order of 4 %.

3. Results and discussion

Modeling the precipitation of phases during the crystallization of the studied system in the temperature range of 1600–20°C showed that for the system under consideration, the most probable is the precipitation of the main phases in the following order: carbides of the MC type; γ — solid solution; eutectic $\gamma + \gamma'$; intermetallic compounds of the γ'-phase type based on (Ni_3Al); carbides of the $M_{23}C_6$ type. A very important parameter during heat treatment is the temperature of the carbide liquidus, which also affects the operating temperatures of the parts. In the work, thermodynamic modeling of the composition of carbides and temperatures of carbide liquidus was carried out, depending on the content of elements in the alloy; on this basis, new mathematical models were developed (Table 1).

In the structure, the volume fractions of both primary MC carbides and secondary carbides $M_{23}C_6$ depend on the carbon con-

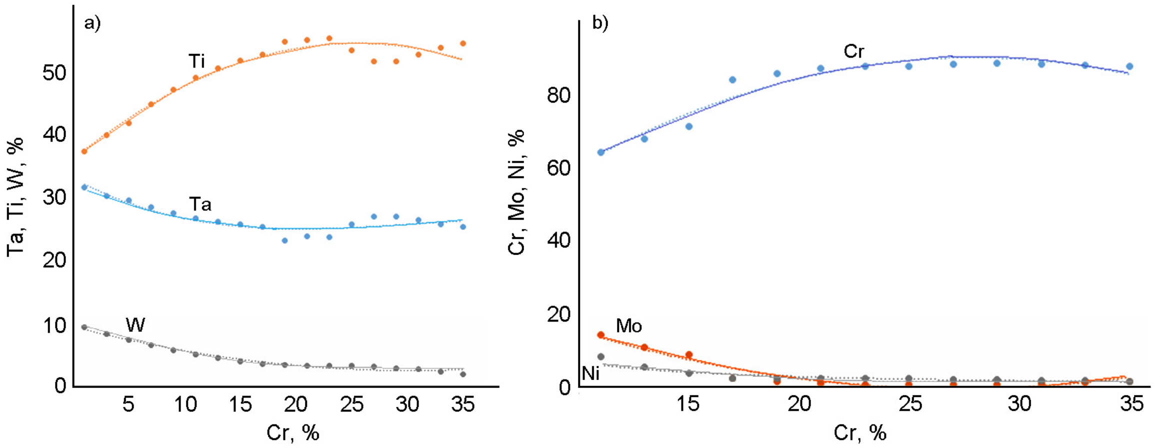

Fig. 1 - Amount of tantalum, titanium and tungsten in the MC carbide (a); chromium, molybdenum and nickel in $M_{23}C_6$ carbide (b) on the chromium content in the alloy.

tent in the alloy composition; the dependences are optimally described by linear functions (Table 1). At the same time that the effect of carbon on the temperature t_L^{MC} of dissolution (or precipitation) of carbides is complex and is optimally described by parabolic equations (Table 1).

It is known [14, 15] that tantalum has a powerful carbide-forming ability and forms primary MC carbides; at the same time, it has a positive effect on both the heat resistance and the corrosion resistance of the liquid pumping station. An increase in the content of tantalum in the alloy leads to an increase in the temperature of the carbide liquidus for the primary carbide and a decrease in the temperature of the secondary carbides, which is described by the following mathematical models (Table 1) With a small introduction of tantalum into the alloy (L≈2%) there is a change in the base of MC carbides from titanium to tantalum (Table 1) to a level of 78%. The transition of MC carbide to tantalum-based carbide leads to an increase in interatomic bonds, which increases the temperature of dissolution (precipitation) of carbide. At the same time, there is a decrease according to the indicated dependences (Table 1), the content of molybdenum and nickel and an increase in the content of tungsten in secondary carbides to a concentration of 6% in the tantalum alloy, higher secondary carbides disappear and the σ-phase is formed.

Titanium is present not only in the composition of the strengthening γ' phase, but is also a strong carbide-forming element on the basis of which MC carbides are formed [16, 17]. It was found that titanium practically does not affect the temperature of dissolution (precipitation) of primary MC carbide up to a concentration of 5.5% (t_L^{MC} = 1325±5°C); at 6%, a sharp jump in t_L^{MC} to 1360°C is observed. However, $t_L^{M_{23}C_6}$ increases in a parabolic dependence up to 971°C (Table 1).

An increase in the titanium content in the alloy leads to an increase in its concentration in the MC carbide up to 28% (Table 1). At the same time, the content of tantalum and hafnium in the carbide decreases to 50% and 6%, respectively. An increase in the concentration of titanium in the alloy leads to a change in the composition of the secondary carbide. An increase in the Ti content leads to an increase in chromium and a decrease in molybdenum and nickel in $M_{23}C_6$.

Hafnium belongs to the elements with a powerful carbide-forming ability, which forms primary carbides in the structure of the superalloys. It was found that hafnium has a significant effect on the temperatures of dissolution (precipitation) of primary carbides according to the parabolic dependence with an extremum at 1.5% Hf. An increase in the temperature of dissolution (separation) of primary carbides at a hafnium concentration of more than 1.5% is associated with the disappearance of secondary carbides at these concentrations.

The composition of primary carbides changes even at a hafnium content of more than 0.5%, the carbides change their base and become hafnium-based carbides. At the same time, the concentration of tantalum and titanium tends to decrease to the level of 8.4% and 0.96%, respectively. In this

Table 1. Dependences of the temperature of dissolution (precipitation) of carbides and the content of alloying elements in carbides on the content of alloying elements in the alloy

Alloying element	Dissolution (precipitation) temperatures of carbides, °C	The amount of carbides (V) and the content of elements in carbide (C), wt.%
C	t_L^{MC}, °C = $5217.8(C)^2 - 152.16\,(C) + {}$ $+1290.6$ $t_L^{M_{23}C_6}$, °C = $-455.49(C)^2 + {}$ $+196.66(C) + 944.85$	$V_{\mathrm{MC}} = 8.9545(C) + 0.048$ $V_{M_{23}C_6} = 19.758(C) + 0.0033$
Ta	t_L^{MC}, °C = $1.2896\cdot(C_{\mathrm{Ta}})^2 - 0.4279(C_{\mathrm{Ta}}) + 1319.9$ $t_L^{M_{23}C_6}$, °C = $-8.8924(C_{\mathrm{Ta}}) + 985.74$	carbides MC: $C_{\mathrm{Ta}} = 22.966\ \ln(C_{\mathrm{Ta}}$ in alloy$) + 25.405$; $C_{\mathrm{Ti}} = -14.77\ \ln(C_{\mathrm{Ta}}$ in alloy$) + 42.121$; $C_{\mathrm{W}} + 5.223.\ln(C_{\mathrm{Ta}}$ in alloy$) + 11.633$ carbides $\mathrm{M_{23}C_6}$: $C_{\mathrm{Mo}} = -0.3875(C_{\mathrm{Ta}}$ in alloy$) + 10.933$; $C_{\mathrm{Ni}} = -0.5677(C_{\mathrm{Ta}}$ in alloy$) + 6.2122$; $C_{\mathrm{W}} = 0.5305(C_{\mathrm{Ta}}$ in alloy$) + 6.6377$
Ti	$t_L^{M_{23}C_6}$, °C = $1.8228(C_{\mathrm{Ti}})^2 - 5.8326\,(C_{\mathrm{Ti}}) + 941.89$	carbides MC: $C_{\mathrm{Ta}} = -11.4\ \ln(C_{\mathrm{Ti}}$ in alloy$) + 69.654$; $C_{\mathrm{Ti}} = 11.515\ \ln(C_{\mathrm{Ti}}$ in alloy$) + 7.1463$; $C_{\mathrm{Hf}} = -1.1142(C_{\mathrm{Ti}}$ in alloy$) + 12.883$ carbides $\mathrm{M_{23}C_6}$: $C_{\mathrm{Cr}} = 2.2036(C_{\mathrm{Ti}}$ in alloy$) + 58.996$; $C_{\mathrm{Mo}} = -1.1327(C_{\mathrm{Ti}}$ in alloy$) + 15.379$; $C_{\mathrm{Ni}} = -1.8136(C_{\mathrm{Ti}}$ in alloy$) + 13.48$
Hf	t_L^{MC}, °C = $6.6787\cdot(C_{\mathrm{Hf}})^2 - 14.897(C_{\mathrm{Hf}}) + 1324.4$	carbides MC: $C_{\mathrm{Hf}} = -13.632(C_{\mathrm{Hf}}$ in alloy$)^2 + 68.388(C_{\mathrm{Hf}}$ in alloy$) - 2.0824$ $C_{\mathrm{Ta}} = -19.422(C_{\mathrm{Hf}}$ in alloy$) + 53.26$ $C_{\mathrm{Ti}} = -8.712\ln(C_{\mathrm{Hf}}$ in alloy$) + 7.2642$
Cr	t_L^{MC}, °C = $-2.7917\cdot(C_{\mathrm{Cr}}) + 1360.8$ (before 17 % Cr in alloy); t_L^{MC}, °C = $-0.1144\cdot\,(C_{\mathrm{Cr}})^2 + 5.9141\cdot(C_{\mathrm{Cr}}) + 1244.1$ (more 17 % Cr in alloy); $t_L^{M_{23}C_6}$, °C = $-0.6732\ \cdot(C_{\mathrm{Cr}})^2 + 33.113\cdot(C_{\mathrm{Cr}}) + 623$	carbides MC: $C_{\mathrm{Ta}} = -0.0284(C_{\mathrm{Cr}}$ in alloy$)^2 + 1.4449(C_{\mathrm{Cr}}$ in alloy$) + 36.265$; $C_{\mathrm{Ti}} = -0.0004(C_{\mathrm{Cr}}$ in alloy$)^3 + 0.0352(C_{\mathrm{Cr}}$ in alloy$)^2 - 0.9489\ (C_{\mathrm{Cr}}$ in alloy$) + 33.149$; $C_{\mathrm{W}} = 0.0075(C_{\mathrm{Cr}}$ in alloy$)^2 - 0.4585(C_{\mathrm{Cr}}$ in alloy$) + 9.5723$; carbides $\mathrm{M_{23}C_6}$: $C_{\mathrm{Cr}} = -0.0918(C_{\mathrm{Cr}}$ in alloy$)^2 + 5.1286(C_{\mathrm{Cr}}$ in alloy$) + 18.728$; $C_{\mathrm{Mo}} = 0.0533(C_{\mathrm{Cr}}$ in alloy$)^2 - 2.9042(C_{\mathrm{Cr}}$ in alloy$) + 38.933$; $C_{\mathrm{Ni}} = 132(C_{\mathrm{Cr}}$ in alloy$)^{-1.299}$
Mo	t_L^{MC}, °C = $1.5804\cdot(C_{\mathrm{Mo}})^2 - 10.063\cdot(C_{\mathrm{Mo}}) + 1332.3$; $t_L^{M_{23}C_6}$, °C = $-1.655(C_{\mathrm{Mo})}^2 + 19.421(C_{\mathrm{Mo}}) + 938.16$	carbides M23C6: $C_{\mathrm{Cr}} = -2.989\ \ln(C_{\mathrm{Mo}}$ in alloy$) + 70.832$; $C_{\mathrm{Mo}} = -0.5382(C_{\mathrm{Mo}}$ in alloy$)^2 + 5.6303(C_{\mathrm{Mo}}$ in alloy$) + 3.2045$; $C_{\mathrm{W}} = 0.03077(C_{\mathrm{Mo}}$ in alloy$)^2 - 3.6629(C_{\mathrm{Mo}}$ in alloy$) + 12.478$
W	t_L^{MC}, °C = $11.936(C_{\mathrm{W}}) + 1259.4$; $t_L^{M_{23}C_6}$, °C = $18.91\ \ln\cdot(C_{\mathrm{W}}) + 938.12$	carbides MC: $C_{\mathrm{W}} = -0.0562(C_{\mathrm{W}}$ in alloy$)^2 + 1.1139(C_{\mathrm{W}}$ in alloy$) + 0.8015$; $C_{\mathrm{Ta}} = 0.0576(\mathrm{CW}$ in alloy$)^2 - 0.9416(C_{\mathrm{W}}$ in alloy$) + 54.283$; carbides $\mathrm{M_{23}C_6}$: $C_{\mathrm{W}} = 0.0109(C_{\mathrm{W}}$ in alloy$)^3 - 0.3855(C\mathrm{W}$ in alloy$)^2 + 4.4129(C_{\mathrm{W}}$ in alloy$) + 2.6308$; $C_{\mathrm{Mo}} = 0.0378(C_{\mathrm{W}}$ in alloy$)^2 - 1.2198(C_{\mathrm{W}}$ in alloy$) + 13.642$

case, the chemical composition of secondary carbides remains practically unchanged.

According to the modeling of crystallization processes, the corresponding dependences of the effect of chromium on the temperatures of dissolution (precipitation) of carbides (Fig. 1) are obtained and are complex and are described by the following equations (Table 1). There is a decrease in the temperature of dissolution (precipitation) of primary carbides up to a concentration of 17 % Cr and an increase up to a concentration of 25 % Cr; this behavior is associated with the precipitation of, respectively, the σ- and α-phase (α–Cr) of the chromium-based solid solution, in the alloy structure. The decrease in $t_L\mathrm{M_{23}C_6}$ over 25 % Cr is explained by a large amount of α–Cr in the alloy structure.

An increase in the chromium concentration in the alloy leads to an increase in the tantalum content in the primary carbide and a decrease in titanium and tungsten (Fig. 1, a) according to complex mathematical relationships (Table 1). In this case, the appearance of secondary carbides is observed with 11% chromium in the alloy, and the composition changes in accordance with the above models (Fig. 1, b) (Table 1).

Molybdenum is one of the elements involved in the formation of secondary carbides of the $\mathrm{M_6C}$ [18] type; in this case, molybdenum can be a part of carbides of the $\mathrm{M_{23}C_6}$ type. Fig. 6 shows that molybdenum has a complex effect on the temperature of dissolution (precipitation) of carbides such as MC and $\mathrm{M_{23}C_6}$. The temperature of dissolution (precipitation) of primary carbides

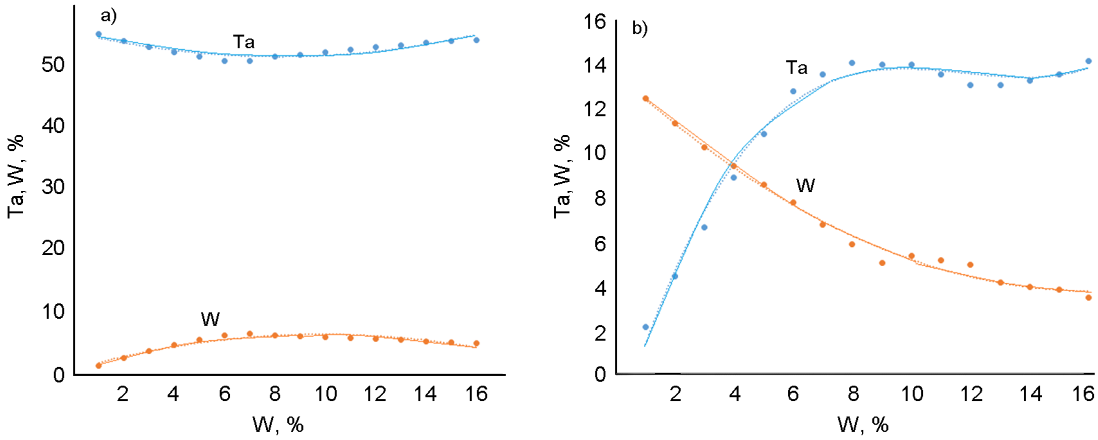

Fig. 2. Amount of tantalum and tungsten in the MC carbide (a); tungsten and molybdenum in $M_{23}C_6$ carbide (b) on the tungsten content in the alloy.

decreases according to a parabolic dependence up to 3.5 % molybdenum (Table 1); this coincides with the concentration for the precipitation of the P-phase; for secondary carbides, an increase in temperature is observed according to a parabolic dependence. An increase in Mo concentration leads to a decrease in chromium and tungsten in the secondary carbide and a simultaneous increase in molybdenum in it (Fig. 6c). This character of the dependences is explained by a change in the forces of interatomic bonds in the secondary carbide (due to an increase in alloying with refractory molybdenum).

Tungsten affects the temperature of dissolution (formation) of MC carbide, starting from 6%, increasing it in direct proportion (this is associated with the formation of the P-phase at the specified concentration) (Fig. 2). The temperature tLM23C6 increases with increasing tungsten concentration. However, W affects the concentration of tantalum and tungsten in the primary carbide according to parabolic dependences (Fig. 2, a). And also, it has a difficult effect on the content of tungsten and molybdenum in secondary carbides (Fig. 2, b), a decrease in the concentration of W at 10% in the alloy is associated with the formation of the σ-phase.

The results of calculating the chemical composition of carbides obtained by the CALPHAD method were further compared with the experimental data obtained using electron microscopy in the microprobe mode on a scanning electron microscope REM-106I. Typical morphology of primary carbides, which is most often found in the structure of alloys of this class in the form of separate blocks (Fig. 3, points 1 and 3). Carbides of the $M_{23}C_6$ type are present in discontinuous block and lamellar forms (Fig. 3, points 2 and 4). The most preferable is the block type of precipitates of secondary carbides, since in this case we have a lower level of stress concentration with the matrix.

The composition of carbides was determined experimentally by X-ray spectral microanalysis (X-ray microanalysis). The presented experimental data agree with the results of thermodynamic calculations obtained by the CALPHAD method. It was experimentally established that the composition of MC carbides includes tantalum, niobium, tungsten, and molybdenum, while the composition of $M_{23}C_6$ carbides contains chromium, tungsten, molybdenum, cobalt, and nickel (Table 2). The errors in determining the elements by this method did not exceed ±1 % (by weight).

Table 2 shows that the calculated and experimental data are in good agreement with each other for almost all elements, the deviation between the calculated and experimental values does not exceed ±3 % by weight.

Based on the obtained experimental values, the stoichiometric formula for carbides was calculated, which made it possible to establish the real type of carbides in the structure of the alloy under study. The stoichiometric formula of primary carbide with conversion from wt.% to atomic % corresponds to the following ratio:

$$(Ta_{0.328}Ti_{0.61}W_{0.019}Hf_{0.04})_{1.03}C_{0.97}.$$

Based on the obtained formula for primary carbides, it follows that the total ratio of metal elements and carbon does not fully

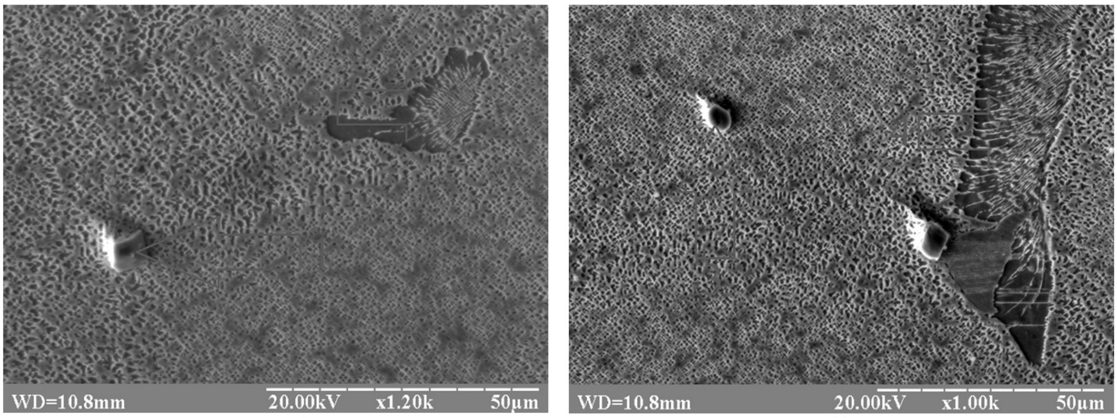

a) b)

Fig. 3. Typical morphology of primary and secondary carbides of the GTD-111 alloy.

Table 2. Chemical compositions of carbides calculated from the obtained dependences and obtained experimentally by the X-ray structural analysis at 20°C of the GTD-111 alloy

Method of obtaining results	Element content, % wt. [at. %]								
	Ta	Ti	W	Mo	Co	Ni	Cr	Hf	C
Calculated MC	51.4	27	4.3	–	–	–	–	7.1	10.2
	[16.1]	[32.04]	[1.32]					[2.25]	[48.23]
Calculated $M_{23}C_6$	–	–	8.3	9.8	2.4	4.4	70.1	–	5.0
			[2.22]	[5,03]	[2]	[3.69]	[66.5]		[20.53]
Experimental MC	53.6 [16.9]	26.3 [31.4]	3.2 [0.99]	–	–	–	–	6.7 [2.14]	10.2 [48.53]
Experimental $M_{23}C_6$	–	–	9.5 [2.57]	10.2 [5.3]	1.9 [1.6]	6.1 [5.18]	67.3 [64.5]	–	5.0 [20.76]

Note — the calculation of stoichiometric formulas for carbides was carried out on the basis of the data given in Table 2 in at.%

comply with the rule of a rigid ratio of 1:1. There is a slight increase in the total concentration of metallic elements. The same feature is observed in carbides of the $M_{23}C_6$ type, it corresponds to the following compound formula:

$$(W_{0.032}Ni_{0.065}Cr_{0.81}Co_{0.02}Mo_{0.066})_{20.7}C_{5.45},$$

which also does not fully comply with the 23:6 ratio rules in carbides of this type.

Thus, the calculated data obtained by the CALPHAD method for determining the type and chemical composition of carbides showed good convergence and agreement with the experimental data obtained by electron microscopy.

4. Conclusions

On the basis of an integrated approach, both computational and experimental, for a multicomponent system, new regression models were obtained that made it possible to solve the problem of computational prediction of the chemical composition of carbides by the chemical composition of the alloy, which was confirmed by the obtained experimental data.

Dependences of the influence of alloying elements on the temperature of dissolution (precipitation) of carbides in the alloy of the Ni–14Cr–9Co–5Ti–3Al–3Ta–3.5W–1.5Mo–0.15Hf–0.1C system have been established. It is shown that the changes in the course of the curves of the temperature dependence on the element content are closely correlated with the thermodynamic processes occurring in the system, that is, extrema are observed on the curves when the stoichiometry of carbides changes or new phases precipitate.

It is shown that with an increase in the total concentration of carbide-forming elements, the chemical composition of carbides also becomes more complex. The introduction of 2 % Ta into the alloy leads to a change in the base of the MC carbide from titanium to tantalum, which leads to an increase in interatomic bonds and an increase in the temperature of the carbide liquidus. At 0.5 % hafnium, the primary carbide changes its base, and at 1.5 % Hf, secondary carbides degenerate in the alloy structure. There is a decrease in the temperature of dissolution (precipitation) of primary carbides up to 17 % Cr and an increase up to a concentration of 25 % Cr; this behavior is associated with the precipitation of the σ-phase and α-phase of the chromium-based solid solution (α–Cr), respectively, in the alloy structure. The temperature of dissolution (precipitation) of primary carbides decreases according to the parabolic dependence up to 3.5 % molybdenum (Table 1) (which coincides with the concentration of precipitation of the P-phase); and for secondary carbides, an increase in temperature is observed according to the parabolic dependence.

A comparative assessment of the calculated results obtained by the CALPHAD method and the experimental data obtained by the X-ray microanalysis was carried out. The results obtained for determining the type and chemical composition of carbides are consistent with each other.

References

1. C.T.Sims, N.S.Stoloff, W.C.Hagel, Superalloys II, John Wiley & Sons, New York (1995). ISBN: 978-0-471-01147-7
2. B.G.Choi, *Solid State Phenomena*, **124–126**, 1505 (2007). https://doi.org/10.4028/www.scientific.net/SSP.124-126.1505
3. A.Mitchell, S.L.Cockcroft, C.E.Schvezov et al., *High Temp. Mater. Proc.*, **15**, 27 (1996). https://doi.org/10.1515/HTMP.1996.15.1-2.27
4. E.Cortes, A.Bedolla-Jacuinde, M.Rainforth et al.. *J. Mater. Eng. Perform*, **28**, 4171 (2019). https://doi.org/10.1007/s11665-019-04179-9
5. A.A.Glotka, S.V.Gaiduk, *J. Appl. Spectr.*, **87**, 812 (2020). https://doi.org/10.1007/s10812-020-01075-2
6. S.Yu.Kondrat'ev, E.V.Sviatysheva, G.P.Anastasiadi et al., *Acta Mater.*, **127**, 267 (2017).
7. P.Jonsta, Z.Jonsta, J.Sojka et al., *J. Achiev. Mater. Manufact. Eng.*, **21**, 29 (2017).
8. Li Jiang, Wen-Zhu Zhang, Zhou-Feng et al., *Mater. & Design*, **112**, 300 (2016), https://doi.org/10.1016/j.matdes.2016.09.075
9. Hu Rui, Li Jinshan, Bai Guanghai, *Mater. Sci. Eng. A*, **548**, 83 (2012). DOI:10.1016/j.msea.2012.03.092
10. A.I.Balitskii, V.I.Vitvitskii, *Proc. of the 2008 Int. Hydrogen Conf. Effects Hydrogen Mater.*, 421 (2009).
11. A.Balitskii, *Proc. Struct. Integrity*, **16**, 134 (2019). https://doi.org/10.1016/j.prostr.2019.07.032
12. Z.A.Duryagina, V.E.Olshanetskiy, Yu.I.Kononenko, Izd. Lviv Politehniky, Lviv (2013).
13. N.Saunders, M.Fahrmann, C.J.Small, *Superalloys 2000 TMS, Warrendale*, 803 (200).
14. M.F.Moreira, L.B.Fantin, F.Beneduce Neto et al., *Inter. Metalcast* (2020). https://doi.org/10.1007/s40962-020-00540-0
15. V.V.Gayduk, B.S.Natapov, V.E.Olshanetskiy, *Fiz. Metal. Metallov.*, **26**, 853 (1968).
16. Z.Hu, C.Qin, X.Chen et al., *Int. J. Precis. Eng. Manuf.*, **21**, 1421 (2020). https://doi.org/10.1007/s12541-020-00347-3
17. O.A.Glotka, S.V.Haiduk, *Metallofiz. Noveishie Tekhnol.*, **42**, 869 (2020). DOI:10.15407/mfint.42.06.0869
18. M.Taheri, A.Halvaee, S.F.Kashani-Bozorg, *Met. Mater. Int.*, (2019). https://doi.org/10.1007/s12540-019-00465-2